Experimental Investigation of Post-fire Mechanical Properties of Cold-formed Steels

Shanmuganathan Gunalan[1] and Mahen Mahendran[2]

Abstract: Cold-formed steel members are widely used in residential, industrial and commercial buildings as primary load-bearing elements. During fire events, they will be exposed to elevated temperatures. If the general appearance of the structure is satisfactory after a fire event then the question that has to be answered is how the load bearing capacity of cold-formed steel members in these buildings has been affected. Hence after such fire events there is a need to evaluate the residual strength of these members. However, the post-fire behaviour of cold-formed steel members has not been investigated in the past. This means conservative decisions are likely to be made in relation to fire exposed cold-formed steel buildings. Therefore an experimental study was undertaken to investigate the post-fire mechanical properties of cold-formed steels. Tensile coupons taken from cold-formed steel sheets of three different steel grades and thicknesses were exposed to different elevated temperatures up to 800 ^{o}C, and were then allowed to cool down to ambient temperature before they were tested to failure. Tensile coupon tests were conducted to obtain their post-fire stress-strain curves and associated mechanical properties (yield stress, Young's modulus, ultimate strength and ductility). It was found that the post-fire mechanical properties of cold-formed steels are reduced below the original ambient temperature mechanical properties if they had been exposed to temperatures exceeding 300 ^{o}C. Hence a new set of equations is proposed to predict the post-fire mechanical properties of cold-formed steels. Such post-fire mechanical property assessments allow structural and fire engineers to make an accurate prediction of the safety of fire exposed cold-formed steel buildings. This paper presents the details of this experimental study and the results of post-fire mechanical properties of cold-formed steels. It also includes the results of a post-fire evaluation of cold-formed steel walls.

Keywords: *Cold-formed steel structures, Post-fire mechanical properties, Exposed temperatures, LSF walls and floors.*

Corresponding author's email address: m.mahendran@qut.edu.au

1 - Research Associate, Science and Engineering Faculty, Queensland University of Technology, Brisbane, QLD 4000, Email: s.gunalan@qut.edu.au

2 - Professor, Science and Engineering Faculty, Queensland University of Technology, Brisbane, QLD 4000, Email: m.mahendran@qut.edu.au

1.0 Introduction

Cold-formed steel members are commonly used as load bearing studs and joists in light gauge steel frame (LSF) walls and floors lined with plasterboards. Inevitably, they can be exposed to fire events as seen in Figure 1. The temperature rise in cold-formed steel studs and joists under a fire event depends on many parameters such as the fire time-temperature curve, duration of the fire and LSF wall and floor configurations (details of plasterboard linings, insulations and their layouts and stud and joist sections). Recent researches have provided a good understanding of the mechanical properties of cold-formed steels [1-5] and the fire performance of LSF walls [6-10] and floors [11] at elevated temperatures. Upon cooling from elevated temperatures, the plasterboards which protected the cold-formed steel studs and joists can be removed from the steel frames to inspect the damage caused by elevated temperatures. The structural engineer then has to decide if the residual strength of the light gauge steel frame is still adequate for future use by using new plasterboard linings.

The residual strength of hot-rolled structural steel members after fire events was investigated in [12-15] and suitable integrity testing procedures (visual observation, non-destructive testing, destructive testing and rectification) have been developed to verify the adequacy of steel members after being exposed to fire. The primary and most basic form of post-fire integrity evaluation is visual observation prior to the cleaning and removal of furniture and other objects destroyed by the fire. This method is used to identify the location of maximum intensity, as well as temperatures reached during the fire (concrete colour changes, melting glass/plastic etc). Structural members are placed into categories based on their deformation (Category 1: Straight members, Category 2: Noticeably deformed and Category 3: Severely deformed [13]). If a hot-rolled steel member is straight (Category 1), then it is presumed that it has not been exposed to critical temperatures and no metallurgical changes have occurred. Members experiencing minor local deformation (Category 2) are generally structurally adequate despite the occurrence of local buckling. Such member deformations can be usually rectified through heat-straightening works. A decision needs to be made whether it will be repaired or replaced. It is likely that Category 3 members have already failed due to the reduction in strength and stiffness of steel at elevated temperatures. The most common form of non-destructive testing used in post-fire evaluation is the surface hardness test. Rapid cooling of austenite steel (above critical phase change temperature) results in hardened steel [13]. Generally, steel that has reached this temperature would not be able to remain straight

under its own weight, resulting in a Category 3 member. Therefore, the surface hardness test would generally only confirm the results of a visual inspection. Destructive testing involves the removal of a specimen from the damaged steel and the evaluation of physical properties, residual stresses and grain structures. Rectification of the structure involves compiling the results of the integrity testing and evaluating the next stage. It may be necessary for the building to be demolished if the extent of the damage is too great. Otherwise it must be decided whether certain members will be repaired or replaced. The decision to repair or replace members is based on the economy of the exercise, the accessibility of the member and its importance.

Although the behaviour of hot-rolled structural steel members after a fire event was investigated by many researchers [12-15], the behaviour of cold-formed steel members after a fire event has not been investigated yet. There are also no design guidelines in [16,17] for assessing fire exposed cold-formed steel members. As a result of this limited knowledge on the post-fire behaviour of cold-formed steel members, over-conservative decisions are likely to be made in relation to the residual capacities of cold-formed steel members after fire events. Improved knowledge of these capacities would help engineers make the right decisions. After a fire event, the exposure to extreme temperature variations could have reduced the section and member load bearing capacities of steel members. The main reason for this is the reduction in post-fire mechanical properties (yield strength, elastic modulus, ultimate strength and ductility) of steels.

Current design standards [16,17] do not provide any information on the mechanical properties of cold-formed steels after being exposed to elevated temperatures. Qiang et al. [18] investigated the post-fire mechanical properties of high strength structural steels (S460 and S690) and proposed suitable predictive equations. Outinen and Makelainen [1] also conducted research on various structural steels and reported some post-fire mechanical properties. Hence this paper investigates the residual mechanical properties of cold-formed steels after being exposed to elevated temperatures, and proposes new equations to predict them. Information gained from this research on post-fire mechanical properties will assist engineers in assessing the axial and bending capacities of fire exposed cold-formed steel members prone to various buckling modes while also enabling further development of the

cold-formed steel design standards with regards to post-fire cold-formed steel member assessments.

2.0 Previous Studies on Post-fire Mechanical Properties

Outinen and Makelainen [1] conducted an experimental study to determine the mechanical properties of S355 cold-formed steels (nominal yield strength of 355 MPa) at elevated temperatures and after cooling. The specimens were taken from SHS 50x50x3 tubes after they had been tested at elevated temperatures. The average measured yield strength of the steel before the elevated temperature tests was 529 MPa. The mechanical properties of fire exposed cold-formed steels were compared with the original measured values at ambient temperature. Figures 2(a) and (b) present the results as the reduction factor versus exposed temperature where the reduction factor was defined as the ratio of the residual ambient temperature mechanical properties. A noticeable decrease in yield strength was observed along with a decreased elastic modulus. However, the yield strength of S355 steel did not reduce below the nominal value of 355 MPa even after being exposed to 700 ^{o}C.

An experimental investigation was performed by Qiang et al. [18] to evaluate the post-fire mechanical properties of high strength structural steels. Two high-strength steel grades, S460 and S690, were investigated in this study (Figures 2(a) to (c)). Their study revealed that steels exposed to low temperatures experienced no change in their elastic modulus compared to ambient temperature. Both steel grades (S460 and S690) almost fully regained their elastic modulus when exposed to temperatures less than 600 ^{o}C. However, a significant degradation of elastic modulus was experienced for specimens exposed to temperatures exceeding 600 ^{o}C. Furthermore, the higher strength (S690) steel experienced greater losses than the lower strength (S460) specimens. The quenched and tempered condition for manufacturing S690 is responsible for the difference of residual elastic modulus between S460 and S690. It was also found that both steel grades regained more than 75% of its elastic modulus when exposed to temperatures up to 800 ^{o}C, and more than 60% when exposed to temperatures up to 1000 ^{o}C.

Similar to the results for elastic modulus, specimens exposed to low temperatures experienced no change in yield strength compared to ambient temperature [18]. The yield strength of both grade steels remained almost unchanged when exposed to temperatures below 600 ^{o}C. It can also be seen that S460 grade steel regained 75% of the yield strength

after being exposed to 1000 ^{o}C while S690 grade steel regained only 38%. The reduction in ultimate strength follows a similar trend to that observed for yield strength. All the test specimens underwent necking before fracture. Ductile failure occurred regardless of the exposed temperature. It was observed that heating of S690 grade specimens improved their ductility in comparison to the ambient temperature specimens.

3.0 Experimental Investigation

Qiang et al.'s [18] study was limited to high strength structural steels and hence this research was conducted on cold-formed steels to investigate the effects of fire on their mechanical properties. An experimental study was undertaken to determine the post-fire mechanical properties of cold-formed steels. Tensile coupon tests were conducted on three different cold-formed steel grades and thicknesses (G300-1.00 mm, G500-1.15 mm and G550-0.95 mm) to obtain their residual stress-strain curves and mechanical properties (elastic modulus, yield stress and ultimate strength) after being exposed to pre-selected temperatures up to 800 ^{o}C. In this experimental study, cold-formed steel specimens were heated to pre-determined temperatures and then allowed to cool down to ambient temperature. A tensile load was then applied to each specimen at a constant strain controlled rate until failure.

3.1. Test Specimens

Test specimens were cut in the longitudinal direction of cold-formed steel sheets. Their shapes and sizes were in accordance with AS 1391 [19] (Figure 3). The base metal thickness and width of each specimen were measured at three points within the gauge length using a micrometer and a vernier calliper, respectively. The averages of these measured dimensions were used in the calculations of mechanical properties.

3.2. Test Set-up and Procedure

The electric furnace shown in Figure 4 was used in this experimental study to achieve the desired elevated temperatures. The thermocouple located inside the furnace gave the air temperature of the furnace on the display. Two additional thermocouples were placed inside the furnace to measure the temperature independently. Ten different temperatures were selected in this study: 20, 300, 400, 500, 550, 600, 650, 700, 750 and 800 ^{o}C. The cold-formed steel becomes very soft at temperatures above 800 ^{o}C and hence temperatures higher than 800 ^{o}C were not considered in this study. Initially, the specimens were placed inside the

furnace using paper clips as props. The furnace temperature was then increased to a temperature 50 ^{o}C less than the pre-selected target value using a heating rate of 10 - 20 ^{o}C/min. After reaching this temperature, it was left for 15 minutes to ensure a uniform temperature distribution. The furnace was then set to a temperature 10 ^{o}C less than the target temperature and left again for 15 minutes. Finally the furnace was set to the target temperature and left for an additional 20 - 30 minutes. This method was followed to prevent any over shooting of the target temperature. The specimens were then removed from the furnace and placed in a tray to air cool at its own rate. The specimens were treated with diluted hydrochloric acid to remove any oxide and coatings that formed on the steel surface. Thereafter strain gauges were attached to measure the strain during the tensile coupon test.

Figure 5 shows the tensile specimen mounted in an Instron testing machine. The specimen was connected to the top and bottom grips, which were accurately aligned with each other. The bottom end was fixed while the top end was free to move upwards. A tensile load was then applied at a constant strain rate until failure. The displacement rate used was 1 mm/min, which satisfied the requirement of AS 1391 [19]. The applied load was measured using a load cell of 50 kN attached to the Instron testing machine. The lab view system was used as the data logger to record the load, displacement and strain gauge measurements.

4.0 Results and Discussions

4.1. Visual Observations

Figure 6 shows the test specimens after being exposed to different elevated temperatures. Cold-formed steel specimens deteriorated quite steadily up to 500 ^{o}C. Beyond this temperature, the effect of heat caused visible damage to steel specimens. For exposed temperatures above 600 ^{o}C, flaking was observed in the form of oxide for high grade steels (G500 and G550). This oxide would be a useful indicator for approximate fire intensity in a practical scenario. The G300 steel specimens became quite abrasive around the edges from approximately 500 ^{o}C onwards and did not show any signs of oxide formation or flaking. With increasing temperatures (700 ^{o}C and above), all the test specimens became quite soft. Figure 7 shows the failed steel specimens after the tensile load tests.

4.2. Stress-strain Curves

Figures 8(a) to (c) show the comparison of stress-strain curves for G300-1.00 mm, G500-1.15 mm and G550-0.95 mm cold-formed steels after being exposed to temperatures in the range of 20 to 800 ^{o}C. The stress-strain curves of both low and high grade steels show a linear elastic region followed by a well-defined yield plateau at ambient and different exposed temperatures. The heat exposed low grade steel specimens follow a similar stress-strain curve as the ambient temperature specimen. On the other hand, the G500 specimens' stress-strain curves differ quite considerably with respect to exposed temperatures. The plastic region is longer for the exposed temperature of 550 ^{o}C, and further extended considerably for temperatures of 600 ^{o}C and above, ie. more ductile after being exposed to higher temperatures. Similar to G500 steel specimens, the stress-strain curves of G550 steel specimens also significantly changed with respect to exposed temperatures and the plastic region extended considerably for higher temperatures (550 ^{o}C and above). This indicates that this trend is expected in higher grade steels exposed to elevated temperatures.

4.3. Elastic Modulus

Elastic modulus was calculated from the initial slope of the stress–strain curve as shown in Figure 9. The elastic modulus reduction factor for exposed temperatures was then calculated as the ratio of the residual elastic modulus of steel after being exposed to an elevated temperature (T) E_T to the original elastic modulus at ambient temperature E. These factors are given in Table 1 and are also plotted in Figure 10(a) as a function of exposed temperature. Figure 10(a) demonstrates that the yield strength reduction characteristics of low (G300) and high grade steels (G500 and G550) are different. Elastic modulus remained relatively unchanged up to 700 °C for low grade cold-formed steel with only slight variations within ±1%. There was a 4% reduction in elastic modulus for low grade steel at 800 ^{o}C. This suggests that low grade steel does not lose its stiffness even after being exposed to high temperatures in a fire. However, the elastic modulus of high grade steel specimens decreased at a higher rate than for low grade steel specimens after being exposed to elevated temperatures. This is similar to the outcome obtained by Qiang et al. [18] for high strength structural steels. There was almost no change in the elastic modulus of high grade cold-formed steels for temperatures up to 400 °C. It then steadily decreased by 15% as the exposed temperature increased to 800 °C.

4.4. Yield Strength

Although there was a clearly defined yield plateau, the yield strength was determined using the 0.2% proof stress method for both low and high grade steels. In addition, the stresses at 0.5%, 1.5% and 2.0% strain levels were also determined from the intersection of stress–strain curve and a non-proportional vertical line at the specified strain values (Figure 9). The yield strength reduction factors for exposed temperatures were calculated as the ratio of the residual yield strength after being exposed to an elevated temperature (T) f_{yT}, to the original yield strength at ambient temperature, f_y. These factors are given in Table 2 and are also plotted in Figure 10(b) as a function of exposed temperature.

Figure 10(b) demonstrates that the yield strength reduction characteristics of low (G300) and high grade steels (G500 and G550) are different, which is similar to the outcome obtained by Qiang et al. [18] for high strength structural steels. The yield strengths of high grade cold-formed steels did not decrease much up to 300 ^{o}C. High grade steels lost their yield strength more rapidly than low grade steels in the exposed temperature range of 500 - 600 ^{o}C with a strength reduction of approximately 60%. The yield strength reduced gradually after this temperature up to 800 ^{o}C. In contrast, the yield strength of low grade steel reduced even for 300 °C showing an initial strength decrease of 8%. Low grade steels lost their yield strengths at a lower rate up to 650 ^{o}C and thereafter decreased at a rapid rate. The low grade steel yield strength decreased by 40% for 800 ^{o}C compared to the ambient temperature yield strength.

4.5. Ultimate Strength

The ultimate strength reduction factors were calculated based on the ratio of the residual ultimate strength after being exposed to an elevated temperature (T) f_{uT} to the original ultimate strength at ambient temperature f_u. These factors are given in Table 3 and are also plotted in Figure 11(c) as a function of exposed temperature. The reduction in ultimate strength follows a similar trend to that observed for yield strength. However, the reduction in ultimate strength was less than the reduction in yield strength for both low and high grade steels as shown in Figures 11(b) and (c).

4.6. Ductility

Ductility of steel is defined based on the level of deformation that steel can undergo plastically before fracture. In this study, tensile strains were measured until fracture and the

resulting stress–strain curves are plotted in the same graph for different exposed temperatures in Figures 8(a) to (c) for G300-1.00, G500-1.15 and G550-0.95 steels, respectively. Effects of exposed temperature and steel grade on the ductility of steel were studied by comparing the strain values at fracture. Low grade steel (G300) shows considerably higher ductility than high grade steels (G500 and G550) at ambient temperature. This can be attributed to the comparatively high strain hardening caused by cold working in the case of high grade steels. Low grade steel gained further ductility when exposed to temperatures in the range of 300 - 600 ^{o}C while its ductility decreased beyond 600 ^{o}C. The ductility of high grade steels remained low for exposed temperatures below 500 ^{o}C but increased considerably and reached the same ductility levels as for low grade steels for temperatures beyond 500 ^{o}C. Similar observations were also made by Qiang et al. [18] for high strength structural steels.

Typical failure modes of low and high grade cold-formed steels for different exposed temperatures are shown in Figure 7. Up to 500 ^{o}C, high grade steels showed less ductile failures (brittle with no necking) and thereafter their failures became more ductile. Brittle failure was not seen in G300 steel, which showed ductile behaviour for ambient and exposed temperatures. These observations indicate that ductility of cold-formed steels will improve considerably after being exposed to a fire event.

5.0 Predictive Equations for Post-fire Mechanical Properties

5.1. Elastic Modulus

Experimental results have shown that the elastic modulus reduces when cold-formed steels are exposed to elevated temperatures. As a simple guide, it can be assumed that cold-formed steels can regain 85% of the original elastic modulus after they are exposed to temperatures up to 800 ^{o}C. However, with the availability of accurate elastic modulus reduction factors of different steel grades (G300, G500, and G550) and thicknesses (0.95 - 1.15 mm), it was considered important to develop predictive equations that are suitable for commonly used cold-formed steels in Australia. Qiang et al. [18] developed predictive equations for the elastic modulus reduction factors as a function of exposed temperature for high strength structural steels S460 and S690 (see Figure 10(a)). However, their equations did not accurately predict the elastic modulus reduction factors for cold-formed steels and hence new empirical equations were developed.

Test results from this study showed that steel grade had some influence on the elastic modulus reduction factors. Hence two separate sets of predictive equations were developed for low and high grade steels. There are two main regions in which the elastic modulus reduction factors vary linearly: 700 - 800 ^{o}C for low grade steels and 400 - 800 ^{o}C for high grade steels. Hence linear equations were developed for the two identified temperature regions to predict the elastic modulus reduction factors of low (Equation 1 (b)) and high grade steels (Equation 2 (b)) for exposed temperatures. Figure 11(a) shows that the test results from this study agree well with the proposed equations.

Low Grade Steels

$E_T / E = 1$ $\quad$ $for\ 20 \leq T \leq 700\ ^{o}C$ (1a)

$E_T / E = 1.28 - 0.0004\ T$ $\quad$ $for\ 700 < T \leq 800\ ^{o}C$ (1b)

High Grade Steels

$E_T / E = 1$ $\quad$ $for\ 20 \leq T \leq 400\ ^{o}C$ (2a)

$E_T / E = 1.15 - 0.000375\ T$ $\quad$ $for\ 400 < T \leq 800\ ^{o}C$ (2b)

5.2. Yield Strength

Experimental results have shown that cold-formed steels can regain 80% of the original yield strength after they are exposed to temperatures below 500 ^{o}C. However, predictive equations are useful to calculate the residual yield strength accurately for different exposed temperatures. Comparison of the residual yield strength results obtained from this research and the predicted values from Qiang et al's [18] equations showed that they were unable to predict the yield strength reduction factors of cold-formed steels for exposed temperatures (see Figure 10(b)). Therefore, new predictive equations were proposed for the yield strength reduction factors obtained in this study.

The yield strength of low grade steel steadily decreased as the specimens were exposed to temperatures up to 650 °C. After this temperature, it decreased linearly with respect to exposed temperature. Equations 3(a) and (b) present the proposed equations for the yield strength reduction factors of low grade steels. The predictions from Equations 3(a) and 3(b) are compared with the test results from this study in Figure 11(b). This figure shows that there is good agreement between the proposed equations and the test results. Therefore it is

recommended to use the proposed equations to determine the yield strength reduction factors of low grade cold-formed steels for a given exposed temperature.

Similarly a new set of equations was developed to determine the yield strength reduction factors of high grade steels by considering the test results obtained from this study. The reduction factors of high grade steels show three main regions after 300 ^{o}C: two nonlinear regions (300 – 500 and 500 – 600 ^{o}C) and one linear region (600 – 800 ^{o}C). Three equations were therefore developed to represent them. Equations 4(a) to (d) present the proposed equations for the yield strength reduction factors of high grade steels. In Figure 11(b), the predictions from Equations 4(a) to (d) are compared with the test results from this research. As shown in this figure there is good agreement between the test results of this study and the proposed equations. Therefore it is recommended to use the proposed Equations 4(a) to (d) to determine the yield strength reduction factors of high grade steels for a given exposed temperature.

Low Grade Steels

$f_{yT}/f_y = 1.005 - 0.00024\,T$ for $20 \le T \le 650\,^{o}C$ (3a)

$f_{yT}/f_y = 2.02 - 0.0018\,T$ for $650 < T \le 800\,^{o}C$ (3b)

High Grade Steels

$f_{yT}/f_y = 1$ for $20 \le T \le 300\,^{o}C$ (4a)

$f_{yT}/f_y = -3.5 \times 10^{-6}\,T^2 + 2.15 \times 10^{-3}\,T + 0.67$ for $300 < T \le 500\,^{o}C$ (4b)

$f_{yT}/f_y = 3.8 \times 10^{-5}\,T^2 - 4.63 \times 10^{-2}\,T + 14.52$ for $500 < T \le 600\,^{o}C$ (4c)

$f_{yT}/f_y = 0.63 - 0.00035\,T$ for $600 < T \le 800\,^{o}C$ (4d)

5.3. Ultimate Strength

Equations 5(a) and (b) present the proposed equations for the ultimate strength reduction factors of low grade steels. The predictions from these equations are compared with the test results from this study in Figure 11(c). This figure shows that there is a good agreement between the proposed equations and the test results. Similarly a new set of equations was developed to determine the ultimate strength reduction factors of high grade steels by considering the test results obtained from this study. Similar to the yield strength reduction factors, the ultimate strength reduction factors of high grade steels show three main regions

after 300 °C: two nonlinear regions (300 - 500 and 500 - 600 °C) and one linear region (600 - 800 °C). Three equations were therefore developed to represent them. Equations 6(a) to (d) present the proposed equations for the ultimate strength reduction factors of high grade steels. In Figure 11(c), the predictions from Equations 6(a) to (d) are compared with the test results from this research. As shown in the figure there is a good agreement between the test results of this study and the proposed equations. Therefore it is recommended to use Equations 5(a) and (b), and Equations 6(a) to (d) to determine the ultimate strength reduction factors of cold-formed steels for exposed temperatures.

Low Grade Steels

$f_{uT}/f_u = 1.002 - 0.000104\ T$ for $20 \le T \le 500\ ^oC$ (5a)

$f_{uT}/f_u = 1.114 - 0.00033\ T$ for $500 < T \le 800\ ^oC$ (5b)

High Grade Steels

$f_{uT}/f_u = 1$ for $20 \le T \le 300\ ^oC$ (6a)

$f_{uT}/f_u = -2.5 \times 10^{-6}\ T^2 + 1.45 \times 10^{-3}\ T + 0.79$ for $300 \le T \le 500\ ^oC$ (6b)

$f_{uT}/f_u = 3.8 \times 10^{-5}\ T^2 - 4.57 \times 10^{-2}\ T + 14.24$ for $500 \le T \le 600\ ^oC$ (6c)

$f_{uT}/f_u = 0.56 - 0.0001\ T$ for $600 < T \le 800\ ^oC$ (6d)

5.4. Post-fire Stress-strain Characteristics

It was observed that the residual stress-strain curves of high grade steels can be assumed to be elastic perfect plastic for exposed temperatures of 500 °C and below. The stress-strain curves of high grade steels (exposed temperatures more than 550 °C) and low grade steel (exposed temperatures up to 800 °C) showed a well-defined yield plateau followed by strain-hardening. Hence these residual stress-strain curves are divided into four different regions as shown in Figure 12 and are defined by Equations 7(a) to (d) [20-22].

$\sigma = E_T \varepsilon$ for $0 \le \varepsilon < \varepsilon_{yT}$ (7a)

$\sigma = f_{yT}$ for $\varepsilon_{yT} \le \varepsilon < \varepsilon_{pT}$ (7b)

$\sigma = f_{uT} - (f_{uT} - f_{yT})\left(\frac{\varepsilon_{uT} - \varepsilon}{\varepsilon_{uT} - \varepsilon_{pT}}\right)^{\rho}$ with $\rho = E_{pT}\left(\frac{\varepsilon_{uT} - \varepsilon_{pT}}{f_{uT} - f_{yT}}\right)$ for $\varepsilon_{pT} \le \varepsilon < \varepsilon_{uT}$ (7c)

$\sigma = f_{uT}$ for $\varepsilon_{uT} \le \varepsilon$ (7d)

where E_T is the residual elastic modulus (Equations 1 and 2);
f_{yT} and f_{uT} are the residual yield and ultimate strengths, respectively (Equations 3 to 6);
ε_{yT} is the yield strain (f_{yT}/E_T);
E_{pT} is the initial elastic modulus at the onset of strain-hardening (Equation 8);
ε_{uT} is the strain at ultimate strength (Equation 9);
ε_{pT} is the strain at the onset of strain-hardening (Equation 10).

In addition to E_T, f_{yT} and f_{uT}, three more parameters (E_{pT}, ε_{uT} and ε_{pT}) are required to define the stress-strain curves of cold-formed steels exposed to elevated temperatures. Figure 13 shows the variation of E_{pT} / E_T with respect to exposed temperatures based on the test results from this study. It can be seen that this ratio increases with increasing exposed temperatures. Hence Equation 8 is proposed to predict this variation. Similarly the variations of $\varepsilon_{uT} / \varepsilon_{yT}$ and $\varepsilon_{pT} / \varepsilon_{yT}$ with respect to exposed temperatures were investigated first. However, a definable relationship was not observed between them. In contrast Figures 14(a) and (b) show a reasonable correlation between $\varepsilon_{uT} / \varepsilon_{yT}$ and $\varepsilon_{pT} / \varepsilon_{yT}$ and the residual yield strength f_{yT}, respectively. It was identified that the two strain ratios decrease with increasing yield strength, based on which suitable predictive equations are proposed (Equations 9 and 10).

$$E_{pT} / E_T = 5.77 \times 10^{-6}\, T + 1.89 \times 10^{-3} \qquad \text{for } 20 \le T \le 800\ ^oC \qquad (8)$$

$$\varepsilon_{uT} / \varepsilon_{yT} = -0.64\, f_{yT} + 338 \qquad \text{for } 200 \le f_{yT} < 450\ MPa \qquad (9)$$

$$\varepsilon_{pT} / \varepsilon_{yT} = -0.132\, f_{yT} + 71.4 \qquad \text{for } 200 \le f_{yT} < 450\ MPa \qquad (10)$$

Figures 15(a) to (c) compare the residual stress-strain curves obtained from tests and Equations 7(a) to (d) for an exposed temperature of 750 ^{o}C. In predicting the stress-strain curves, Equations 1 to 6 and 8 to 10 were used to predict E_T, f_{yT}, f_{uT}, E_{pT}, ε_{uT} and ε_{pT} based on the measured mechanical properties at ambient temperature (E, f_y and f_u). A reasonably good agreement between the stress-strain curves in Figures 15(a) to (c) show that the stress-strain model based on the proposed Equations 7(a) to (d) is able to predict the stress-strain curves of cold-formed steels after being exposed to elevated temperatures.

6.0 Discussion of Results

6.1. Comparison with Elevated Temperature Mechanical Properties

In this section, residual mechanical properties of cold-formed steels following elevated temperature exposure as obtained from this study are compared with the 'hot' mechanical properties of the same steels at elevated temperatures. For this purpose the elevated temperature mechanical property reduction factor equations proposed by Dolamune Kankanamge and Mahendran [5] are compared with the post-fire mechanical property reduction factor equations developed in this study in Figures 16(a) and (b). These figures show that cold-formed steels regain their mechanical properties to a greater extent even after being exposed to high temperatures. For example, both low and high grade steels retained about 90% of the original (ambient temperature) elastic modulus and yield strength after being exposed to 500 ^{o}C.

The loss in residual elastic modulus for both steels was quite small even at very high exposed temperatures, ie. less than 20% at 800 ^{o}C. For low grade steels the loss in residual yield strength was less than 20% up to 650 ^{o}C. However, high grade cold-formed steels lost suddenly their residula yield strength to about 40% in the temperature region of 500 – 600 ^{o}C. This trend is similar to that seen with elevated temperature yield strength curve.

Elevated temperature yield strength factors are quite small (0.1) at 800 ^{o}C, and at such high temperatures, thin cold-formed steels would have distorted severly. Hence further research on post-fire behaviour is not required beyond 800 ^{o}C for cold-formed steels.

6.2. Post-fire Evaluation of LSF Walls

Recent research at the Queensland University of Technology has investigated the structural and thermal behaviour of load bearing light gauge steel frame (LSF) wall systems made of G500-1.15 mm steel studs and eight plasterboard and insulation configurations (cavity and external insulation) shown in Table 4 using full scale fire tests of walls exposed to standard and realistic design fires [6, 23, 24]. Suitable equations were proposed using the measured stud temperatures in these tests to predict the time-temperature distributions of LSF wall studs used with different plasterboard-insulation configurations [9]. This section presents an evaluation of the residual strength of LSF wall studs exposed to standard fires based on these

time-temperature distributions and the post-fire yield strengths reported in the last section. A similar procedure can be used for LSF walls exposed to realistic design fires.

When LSF walls were tested under standard fire conditions [6], the maximum (hot flange) temperatures of the steel stud were 20 ^{o}C for the initial few minutes. They then increased gradually to reach 100 ^{o}C and remained at the same temperature during the plasterboard dehydration process. After this the steel temperatures increased rapidly with time. Table 4 shows the time-temperature distributions of hot flange up to 100^{o}C. A linear variation of temperature distribution was assumed between the selected times in Table 4. Beyond 100^{o}C, Equations 11 to 18 represent the idealised time-temperature distributions of the hot flanges of studs in the LSF wall panels with eight configurations shown in Table 4, where T_{HF} is the average hot flange temperature in ^{o}C and t is the time in minutes.

LSF wall lined on both sides by a single layer of plasterboard (1x1)

$T_{HF} = -0.1066t^2 + 20.17t - 165$ *for* $15 \leq t$ (11)

LSF wall lined on both sides by two layers of plasterboard (2x2)

$T_{HF} = 6.35t - 160$ *for* $42 \leq t \leq 110$ (12a)

$T_{HF} = 12.11t - 790$ *for* $110 < t$ (12b)

LSF wall lined on both sides by two layers of plasterboard with glass fibre used as cavity insulation (CI-GF)

$T_{HF} = 11.17t - 490$ *for* $53 \leq t$ (13)

LSF wall lined on both sides by two layers of plasterboard with rock fibre used as cavity insulation (CI-RF)

$T_{HF} = 10.2t - 435$ *for* $53 \leq t$ (14)

LSF wall lined on both sides by two layers of plasterboard with cellulose fibre used as cavity insulation (CI-CF)

$T_{HF} = 8.94t - 360$ *for* $53 \leq t \leq 106$ (15a)

$T_{HF} = 19.83t - 1530$ *for* $106 < t$ (15b)

LSF wall lined on both sides by two layers of plasterboard with glass fibre used as external insulation (CP-GF)

$T_{HF} = 0.001007t^3 - 0.1605t^2 + 12.15t - 205$ *for* $43 \leq t$ (16)

LSF wall lined on both sides by two layers of plasterboard with rock fibre used as external insulation (CP-RF)

$$T_{HF} = -0.000212t^3 + 0.0931t^2 - 5.47t + 100 \qquad for \qquad 71 \leq t \tag{17}$$

LSF wall lined on both sides by two layers of plasterboard with cellulose fibre used as external insulation (CP-CF)

$$T_{HF} = -0.000286t^3 + 0.1024t^2 - 2.92t - 100 \qquad for \qquad 71 \leq t \tag{18}$$

For the purpose of calculating the residual strength of LSF wall studs, Equations 11 to 18 were first used to calculate the hot flange temperatures of G500-1.15 mm steel studs at 10 minute intervals when they were exposed to a standard fire curve. The hot flange temperatures were then used to predict the corresponding residual yield strength factors of steel studs using Equations 4(a) to (d). Table 5 and Figure 17 show the residual yield strength factors of G500-1.15 mm steel studs used in different LSF wall configurations after being exposed to a certain time during a standard fire. Assuming that the compressive strength of stud is directly proportional to the steel yield strength, Table 5 and Figure 17 results can be used to estimate the residual strength of LSF walls after being exposed a fire of certain duration. As shown in Figure 17 the reduction in the strength of wall studs can be therefore estimated for a particular fire exposure time. These results show that the G500-1.15 mm steel studs protected by single layer of plasterboards can be re-used with its original capacity (reduction factor ≈ 1) if the fire exposure time is less than 30 minutes and the distortions of the steel stud are within the tolerance limits. On the other hand if two layers of plasterboards are used in LSF wall construction, the same studs can be re-used with new plasterboards even after 70 minutes of fire exposure. Table 6 presents a summary of fire exposure times for the eight LSF wall configurations considered here to retain the original and 90% strength of steel studs. It demonstrates the possibility of re-using the same steel wall frames with new plasterboard linings and insulations following a fire. The results in Tables 5 and 6 also show that LSF walls with certain configurations such as external rockwool insulations provide a greater chance of re-using the same steel wall frames. Fire exposed LSF wall frames can be re-designed using the post-fire mechanical properties reported in this paper and the design method presented in [25,26] for plasterboard lined LSF walls.

7.0 Conclusions

This paper has presented a detailed experimental study of the post-fire mechanical properties of cold-formed steels. This study included tensile coupon tests conducted on G300-1.00, G500-1.15 and G550-0.95 mm cold-formed steels for an exposed temperature range of 20 -

800 ^{o}C. Test specimens were heated to various elevated temperatures before being allowed to cool down to ambient temperature. The stress-strain curves, yield and ultimate strengths and elastic modulus were determined from the tensile coupon tests. Test results showed that cold-formed steels can regain 85% of the original elastic modulus after they are exposed to temperatures up to 800 ^{o}C. They can also regain 80% of the original yield strength after exposed to temperatures below 500 ^{o}C. The yield strength of high grade steel was significantly reduced after being exposed to temperatures above 500 °C. The results showed that the steel grade had an influence on the yield strength and elastic modulus of steel while there was no observable influence of steel thickness on the results. The reduction in yield strength and elastic modulus of low grade steels were found to be less than that of high grade steels. Neither the current design standards nor the proposals by other researchers provided suitable reduction factors for the residual post-fire mechanical properties of cold-formed steels. Therefore predictive equations were developed for these mechanical properties of low and high grade cold-formed steels as a function of exposed temperature. Finally a post-fire evaluation of LSF walls was conducted using the available hot flange time-temperature profiles from standard fire tests in [6] and the post-fire mechanical properties from this study. It was found that the G500-1.15 mm steel studs protected by single and double layers of plasterboards can be re-used with its original capacity if the fire exposure time is less than 30 and 70 minutes, respectively, and the distortions of the steel studs were within the tolerance limits.

Acknowledgements

The authors would like to thank Australian Research Council for their financial support and the Queensland University of Technology for providing the necessary facilities and support to conduct this research project. They would also like to thank Michael Bardini, Blake Scriven, Daniel Marshall and Wade Gurtner for their assistance with the experimental study reported in this paper.

References

[1] Outinen, J. and Makelainen, P. (2004), Mechanical properties of structural steel at elevated temperatures and after cooling down, Fire and Materials, Vol. 28, pp. 237-251.

[2] Mecozzi, E. and Zhao, B. (2005), Development of stress–strain relationships of cold-formed lightweight steel at elevated temperatures, Proceedings of the EuroSteel Conference, pp. 41-49.

[3] Chen, J. and Young B. (2007), Experimental investigation of cold-formed steel material at elevated temperatures, Thin-Walled Structures, Vol. 45, pp. 96-110.

[4] Ranawaka, T. and Mahendran, M. (2009), Experimental study of the mechanical properties of light gauge cold-formed steels at elevated temperatures, Fire Safety Journal, Vol. 44(2), pp. 219-229.

[5] Dolamune Kankanamge, N. and Mahendran, M. (2011), Mechanical properties of cold-formed steels at elevated temperatures, Thin-Walled Structures, Vol. 49, pp. 26-44.

[6] Gunalan, S., Kolarkar, P.N. and Mahendran, M. (2013), Experimental study of load bearing cold-formed steel wall systems under fire conditions, Thin-Walled Structures, Vol. 65, pp. 72–92.

[7] Gunalan, S. and Mahendran, M. (2013), Finite element modelling of load bearing cold-formed steel wall systems under fire conditions, Engineering Structures, Vol. 56, pp. 1007-1027.

[8] Gunalan, S. and Mahendran, M. (2014), Review of current fire design rules for cold-formed steel wall systems. Journal of Fire Sciences, Vol. 32, Issue 1, pp. 3-34.

[9] Gunalan, S. and Mahendran, M., (2014), Fire performance of cold-formed steel wall panels and prediction of their fire resistance rating, Fire Safety Journal, DOI 10.1016/j.firesaf.2013.12.003.

[10] Gunalan, S. and Mahendran, M. (2013), Development of improved fire design rules for cold-formed steel wall systems, Journal of Constructional Steel Research, Vol. 88, pp.339-362.

[11] Baleshan, B. and Mahendran, M. (2010), Improvements to the fire performance of light gauge steel floor systems, Proceedings of the 20th International Specialty Conference on Cold-formed steel Structures, Missouri, USA, pp. 137-154.

[12] Dill, F.H. (1960), Structural steel after a fire, Proceedings of AISC National Engineering Conference, pp. 78-80.

[13] Tide, R.H.R. (1998), Integrity of structural steel after exposure to fire, Engineering Journal, pp. 26-38.

[14] Chan, D. (2009), Fire damage assessment of structural steel in a school, The Structural Engineer, 87(19), pp.18-20.

[15] Kirby, B.R., Lapwood, D.G. and Thomson, G. (1993), The reinstatement of fire damaged steel and iron framed structures, Technical Report, British Steel Swinden Laboratories, London, UK.

[16] British Standard Institution (BSI) (2003), Structural use of steel work in building. Part 8: Code of practice for fire resistant design, BS 5950-8, London, UK.

[17] European Committee for Standardization (ECS) (2005), Eurocode 3: Design of steel structures. Part 1.2: General rules - Structural fire design, EN 1993-1-2, Brussels.

[18] Qiang, X., Bijlaard, F.S.K. and Kolstein, H. (2012), Post-fire mechanical properties of high strength structural steels S460 and S690, Engineering Structures, Vol. 35, pp. 1-10.

[19] Standards Australia (SA), (2007), Methods for tensile testing of metal, AS 1391, Sydney, Australia.

[20] Wang, X.Q and Tao, Z. and Uy, B. (2012), Stress-strain curves of structural steel after exposure to elevated temperatures, Proceedings of the 10th International Conference on Advances in Steel Concrete Composite and Hybrid Structures, Singapore, pp. 833-840.

[21] Mander, J.B. (1983), Seismic design of bridge piers, PhD Thesis, University of Cantebury, Christchurch, New Zealand.

[22] Boeraeve, Ph., Lognard, B., Janss, J., Gerardy, J.C. and Schleich, J.B. (1993), Elasto-plastic behaviour of steel frame works, Journal of Constructional Steel Research, Vol. 27, pp. 3-21.

[23] Ariyanayagam AD (2013), Fire performance and design of light gauge steel frame wall systems exposed to realistic design fires, PhD Thesis, Queensland University of Technology, Brisbane, Australia.

[24] Ariyanayagam AD and Mahendran M (2014) Numerical modelling of load bearing light gauge steel frame wall systems exposed to realistic design fires. Thin-Walled Structures Vol. 78, pp. 148-170.

[25] Telue, Y. and Mahendran, M. (2001), Behaviour of cold-formed steel wall frames lined with plasterboard, Journal of Constructional Steel Research, Vol.57, pp. 435-452.

[26] Telue, Y. and Mahendran, M. (2004), Behaviour and design of cold-formed steel wall frames lined with plasterboard on both sides, Engineering Structures, Vol.26, pp. 567-579.

Table 1: Post-fire elastic modulus and reduction factors

T (^{o}C)	Elastic modulus (MPa)			Reduction factor		
	G300-1.00	G500-1.15	G550-0.95	G300-1.00	G500-1.15	G550-0.95
20	209053	227096	231575	1.000	1.000	1.000
300	210390	225867	231660	1.006	0.995	1.000
400	212014	225131	230013	1.014	0.991	0.993
500	209532	224223	226776	1.002	0.987	0.979
550	207123	219095	210002	0.991	0.965	0.907
600	210697	216504	209715	1.008	0.953	0.906
650	207576	208246	210482	0.993	0.917	0.909
700	207103	207012	-	0.991	0.912	-
750	205712	203279	205746	0.984	0.895	0.888
800	201516	203440	197724	0.964	0.896	0.854

Table 2: Post-fire yield strengths and reduction factors

Steel	T (^{o}C)	Yield strength (MPa)				Reduction factor			
		0.2%	0.5%	1.5%	2.0%	0.2%	0.5%	1.5%	2.0%
G300-1.00	20	351.5	352.2	352.6	352.6	1.000	1.000	1.000	1.000
	300	324.2	322.6	323.8	323.8	0.922	0.916	0.918	0.918
	400	323.6	320.2	323.2	323.2	0.921	0.909	0.917	0.917
	500	306.5	306.1	303.6	303.6	0.872	0.869	0.861	0.861
	550	300.5	304.1	309.8	309.8	0.855	0.863	0.879	0.879
	600	308.8	310.2	311.7	311.7	0.879	0.881	0.884	0.884
	650	297.1	297.6	298.5	298.5	0.845	0.845	0.847	0.847
	700	254.2	257.1	265.7	265.7	0.723	0.730	0.754	0.754
	750	238.9	238.5	241.3	241.3	0.680	0.677	0.684	0.684
	800	-	-	-	-	-	-	-	-
G500-1.15	20	663.9	664.0	663.9	663.9	1.000	1.000	1.000	1.000
	300	657.3	657.3	657.4	657.4	0.990	0.990	0.990	0.990
	400	651.3	651.3	651.1	651.1	0.981	0.981	0.981	0.981
	500	608.6	608.5	608.8	608.8	0.917	0.916	0.917	0.917
	550	409.1	408.8	408.8	408.8	0.616	0.616	0.616	0.616
	600	286.4	286.0	285.0	285.0	0.431	0.431	0.429	0.429
	650	232.8	232.9	232.1	232.1	0.351	0.351	0.350	0.350
	700	261.7	262.1	262.6	262.6	0.394	0.395	0.395	0.395
	750	246.8	247.2	247.7	247.7	0.372	0.372	0.373	0.373
	800	262.4	264.0	266.6	266.6	0.395	0.398	0.402	0.402
G550-0.95	20	664.4	664.4	644.0	644.0	1.000	1.000	1.000	1.000
	300	671.1	671.1	643.6	643.6	1.010	1.010	0.999	0.999
	400	653.9	653.9	631.7	631.7	0.984	0.984	0.981	0.981
	500	553.3	554.5	556.3	556.3	0.833	0.835	0.864	0.864
	550	309.8	309.2	311.6	311.6	0.466	0.465	0.484	0.484
	600	300.3	300.8	302.7	302.7	0.452	0.453	0.470	0.470
	650	283.2	283.1	282.0	282.0	0.426	0.426	0.438	0.438
	700	-	-	-	-	-	-	-	-
	750	260.6	260.3	260.4	260.4	0.392	0.392	0.404	0.404
	800	241.7	241.7	241.2	241.2	0.364	0.364	0.375	0.375

Table 3: Post-fire ultimate strengths and reduction factors

T (^{o}C)	Ultimate strength (MPa)			Reduction factor		
	G300-1.00	G500-1.15	G550-0.95	G300-1.00	G500-1.15	G550-0.95
20	366.2	668.3	664.4	1.000	1.000	1.000
300	360.4	669.0	675.3	0.984	1.001	1.016
400	357.6	655.2	658.1	0.976	0.980	0.990
500	347.8	615.3	561.1	0.950	0.921	0.845
550	343.2	457.8	352.3	0.937	0.685	0.530
600	338.0	351.2	342.9	0.923	0.526	0.516
650	335.9	320.8	341.8	0.917	0.480	0.514
700	310.8	323.9	-	0.849	0.485	-
750	317.2	325.6	324.7	0.866	0.487	0.489
800	-	327.3	318.4	-	0.490	0.479

Table 4: Idealised time-temperature values up to 100°C

W/C	Index	Configuration	Insulation	Time (min.)	HFT (°C)
1	1 x 1		None	2	20
				6	100
				14	100
2	2 x 2	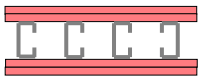	None	2	20
				25	100
				41	100
3	CI-GF	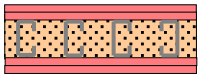	Glass Fibre (GF)	6	20
				20	100
				52	100
4	CI-RF	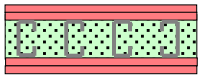	Rock Fibre (RF)	6	20
				25	100
				52	100
5	CI-CF	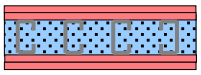	Cellulose Fibre (CF)	6	20
				25	100
				52	100
6	CP-GF	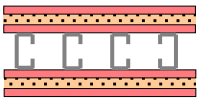	Glass Fibre (GF)	6	20
				40	100
				42	100
7	CP-RF	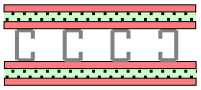	Rock Fibre (RF)	6	20
				55	100
				70	100
8	CP-CF	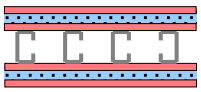	Cellulose Fibre (CF)	6	20
				45	100
				70	100

W/C - Wall Configuration; HFT - Hot Flange Temperature; CI - Cavity Insulation; CP - Composite Panel with External Insulation

Table 5: Residual yield strength factors of G500-1.15 mm steel studs in various LSF wall configurations after a standard fire exposure

Time (min.)	1x1		2x2		CI-GF		CI-RF		CI-CF		CP-GF		CP-RF		CP-CF	
	T (°C)	RF	T (°C)	RF	T (°C)	RF	T (°C)	RF	T (°C)	RF	T (°C)	RF	T (°C)	RF	T (°C)	RF
10	100	1.00	48	1.00	43	1.00	37	1.00	37	1.00	29	1.00	27	1.00	28	1.00
20	196	1.00	83	1.00	100	1.00	79	1.00	79	1.00	53	1.00	43	1.00	49	1.00
30	344	1.00	100	1.00	100	1.00	100	1.00	100	1.00	76	1.00	59	1.00	69	1.00
40	471	0.91	100	1.00	100	1.00	100	1.00	100	1.00	100	1.00	76	1.00	90	1.00
50	577	0.46	158	1.00	100	1.00	100	1.00	100	1.00	127	1.00	92	1.00	100	1.00
53	Failure		177	1.00	102	1.00	106	1.00	114	1.00	138	1.00	93	1.00	100	1.00
60			221	1.00	180	1.00	177	1.00	176	1.00	164	1.00	100	1.00	100	1.00
70			285	1.00	292	1.00	279	1.00	266	1.00	204	1.00	100	1.00	100	1.00
80			348	0.99	404	0.97	381	0.98	355	0.99	255	1.00	150	1.00	175	1.00
90			412	0.96	515	0.75	483	0.89	445	0.93	323	1.00	207	1.00	258	1.00
100			475	0.90	627	0.41	585	0.44	534	0.63	412	0.96	272	1.00	346	0.99
101			481	0.89	Failure		595	0.42	543	0.58	422	0.95	279	1.00	355	0.99
107			519	0.72			Failure		597	0.42	491	0.88	321	1.00	410	0.96
110			539	0.61					651	0.40	530	0.66	343	1.00	437	0.94
111			Failure						Failure		543	0.58	350	0.99	446	0.93
118											Failure		403	0.97	511	0.78
120													418	0.96	530	0.66
124													449	0.93	Failure	
130													497	0.87		
136													Failure			

Table 6: Allowable fire exposure times to retain 90 and 100% of original yield strength

Fire exposure time (minutes)								Residual yield strength
1x1	2x2	CI-GF	CI-RF	CI-CF	CP-GF	CP-RF	CP-CF	
30	70	70	70	70	90	110	90	100%
40	100	80	80	90	100	120	110	90%

(a) Building fire
Image from http://www.firehouse.com/
[Accessed February 10, 2014]

(b) LSF wall after fire

(c) Steel frame after fire

Figure 1: Fire damaged structures

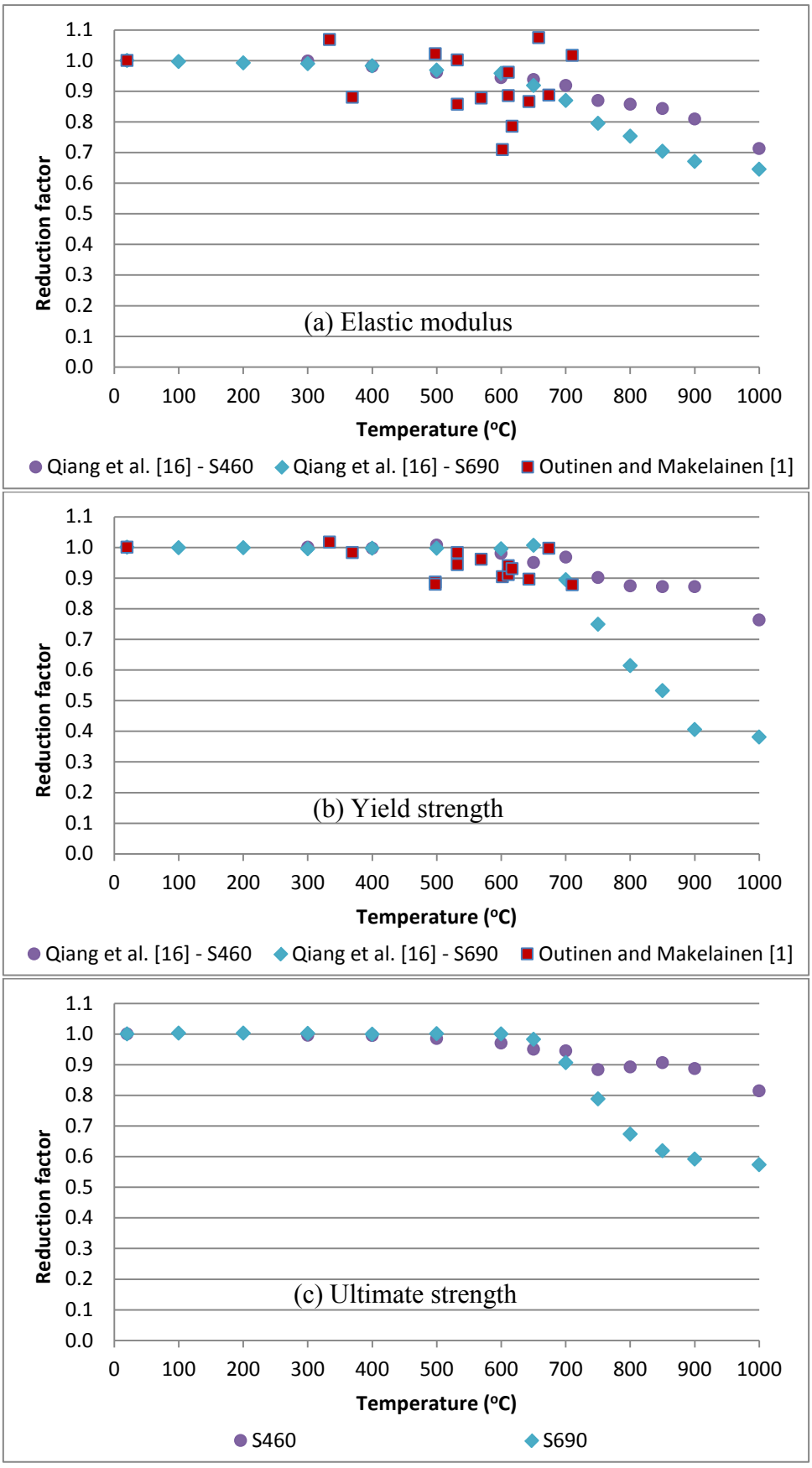

Figure 2: Post-fire mechanical property results from [1] and [16]

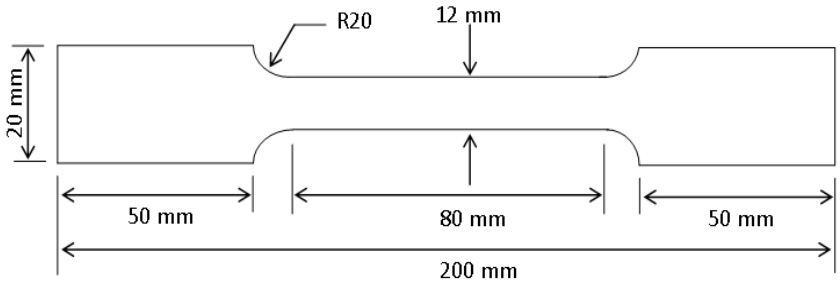

Figure 3: Tensile coupon dimensions

Figure 4: Electric furnace used for heating the test specimens

Figure 5: Tensile test set-up

Figure 6: Test specimens after being exposed to elevated temperatures

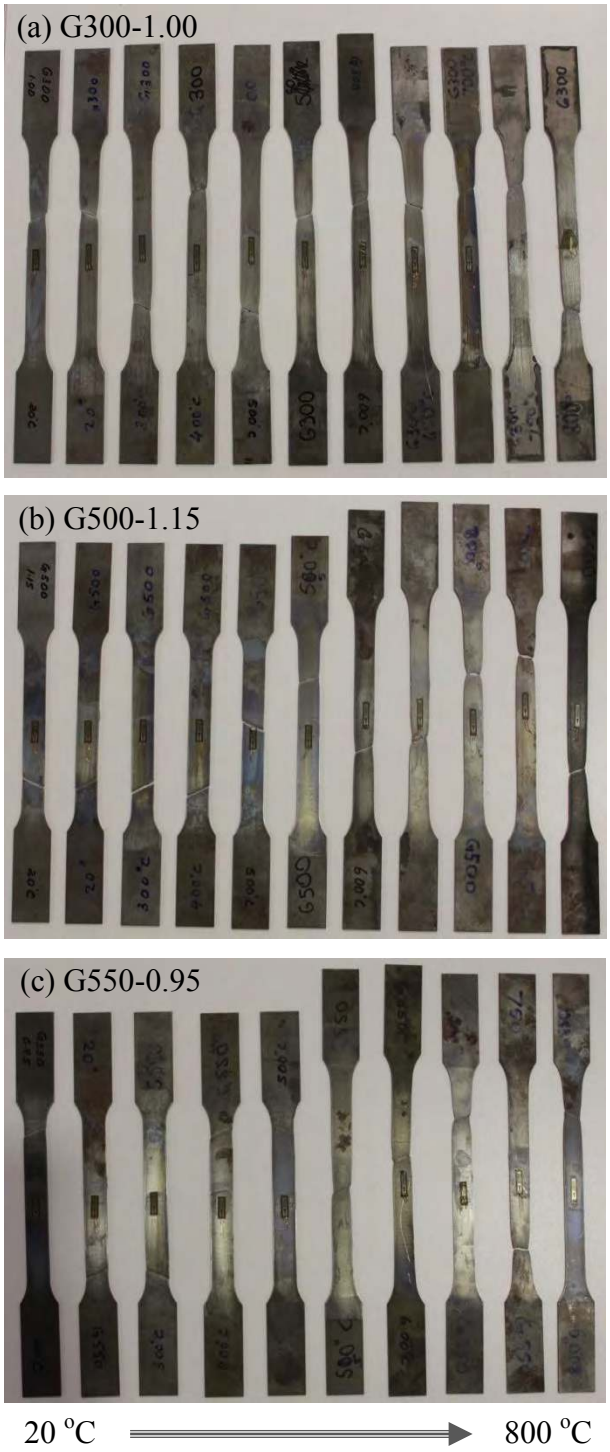

Figure 7: Failure modes of test specimens

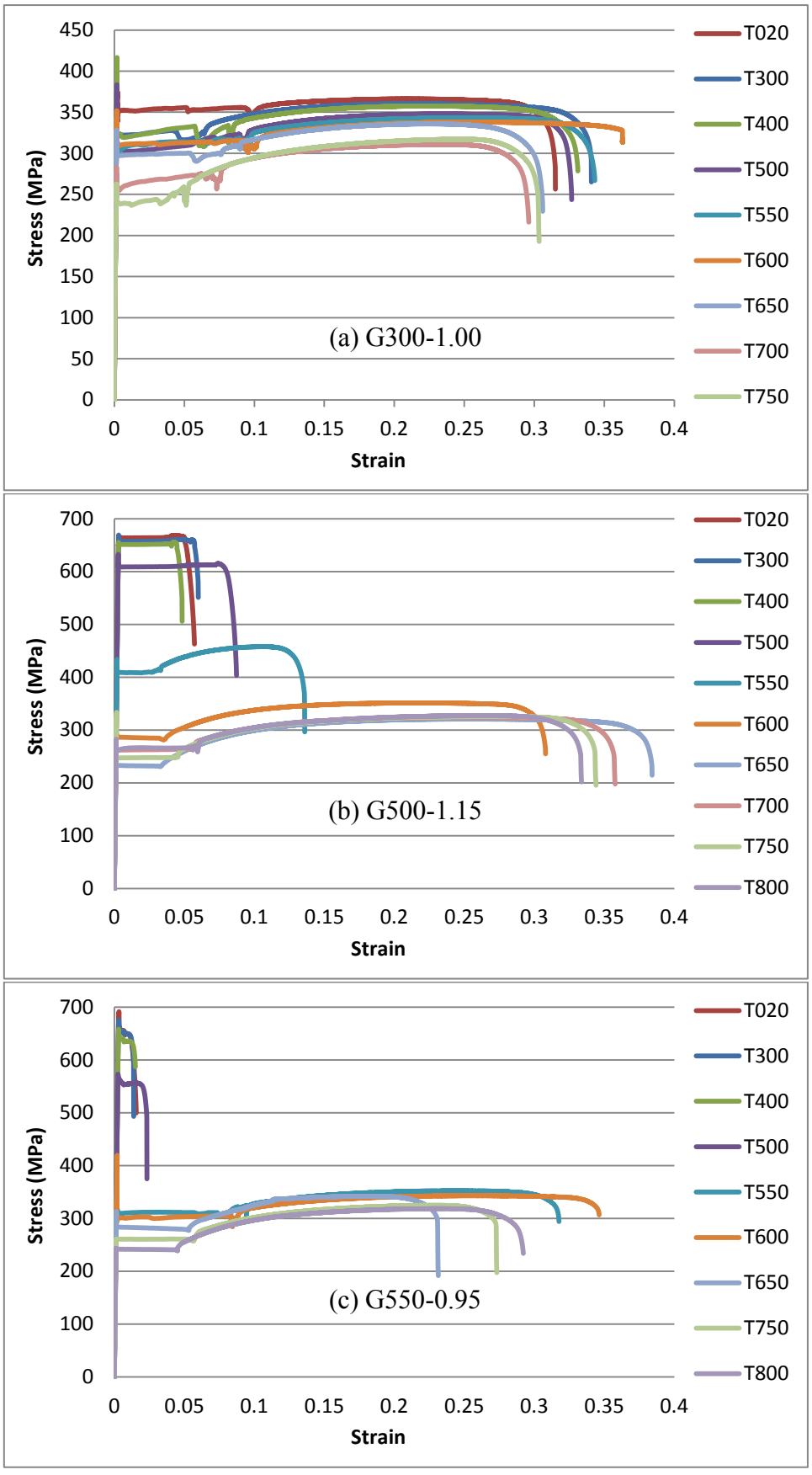

Figure 8: Stress-strain curves for different exposed temperatures

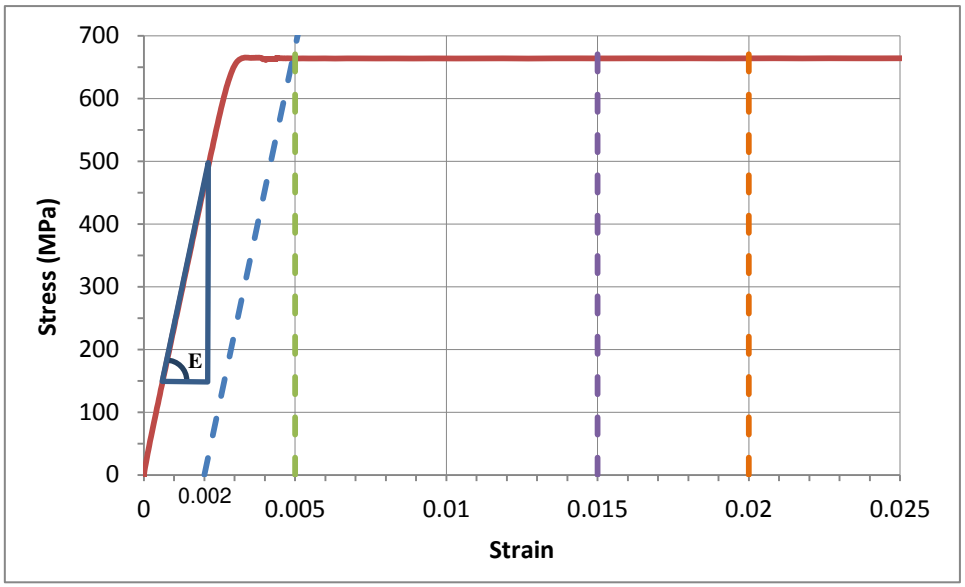

Figure 9: Elastic modulus and yield strength determination

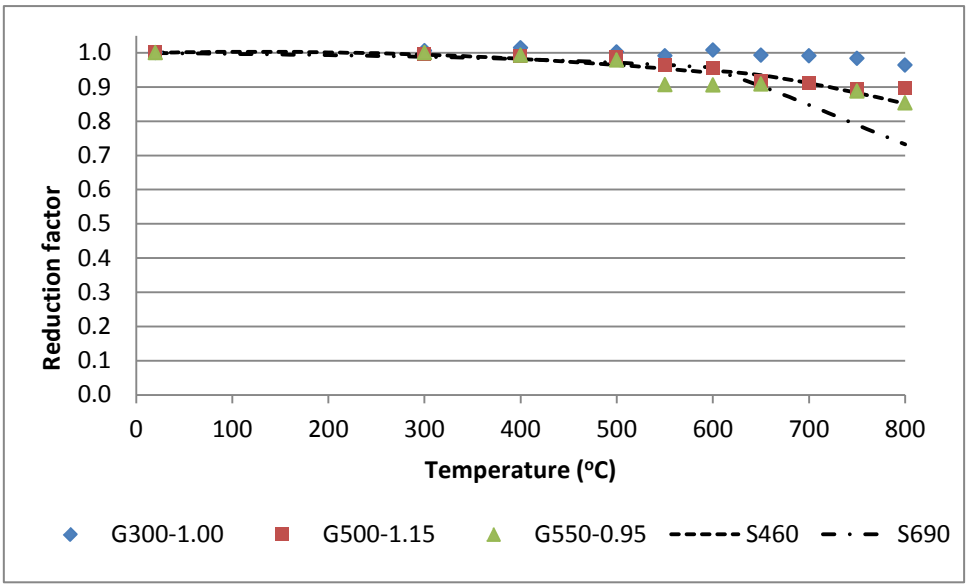

(a) Elastic modulus

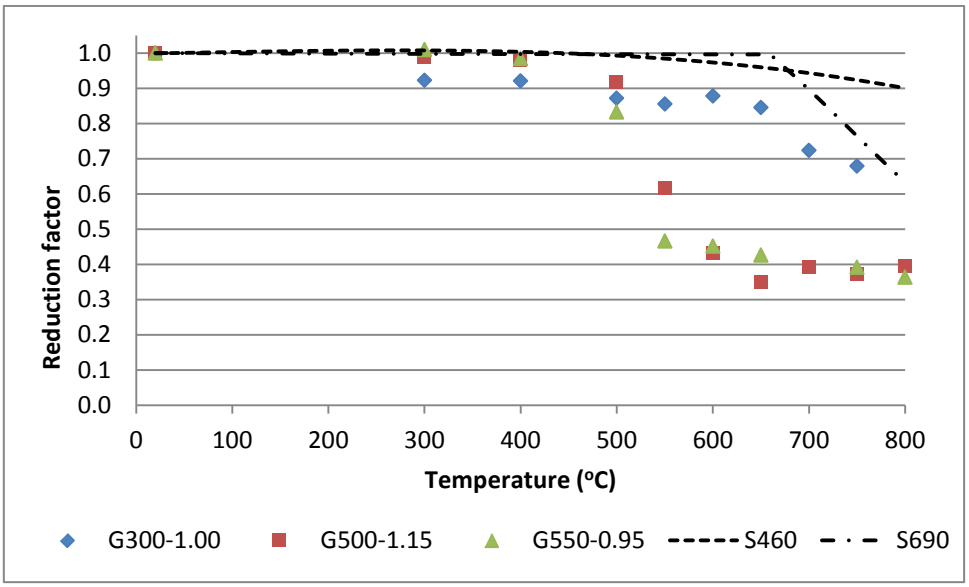

(b) Yield strength

Figure 10: Comparison of test results with Qiang et al.'s [16] predictions

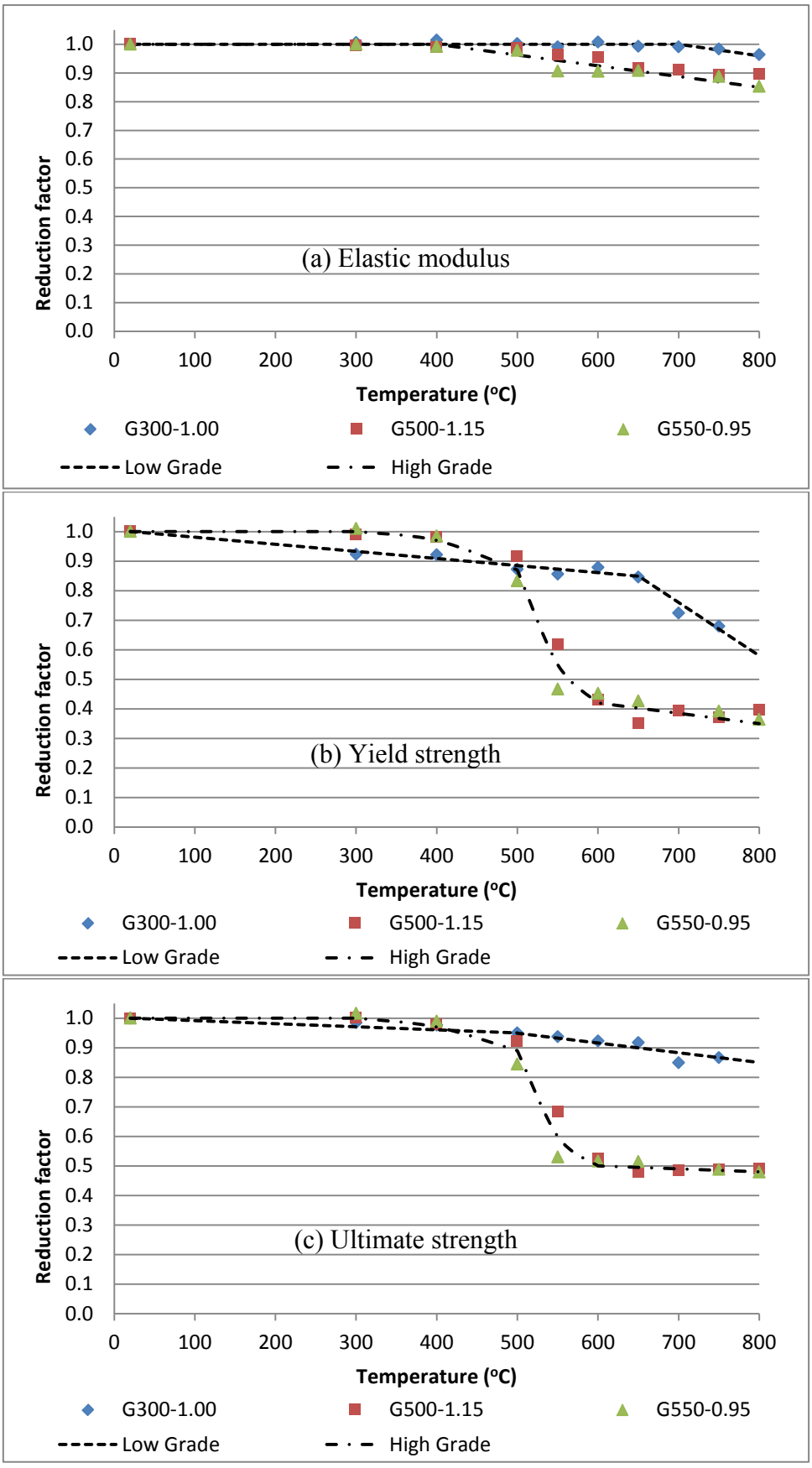

Figure 11: Comparison of test results with predictions

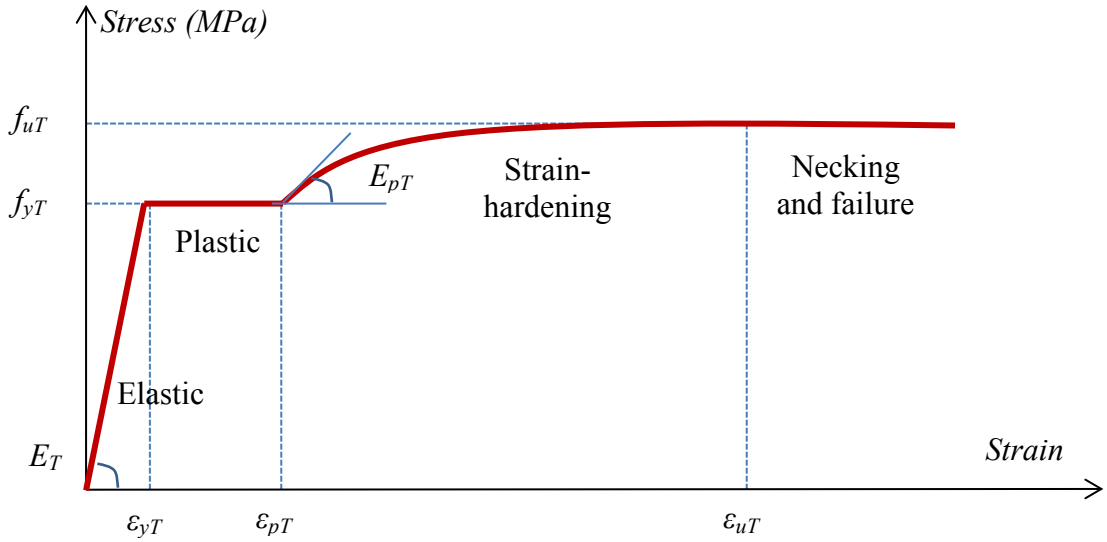

Figure 12: Stress-strain model

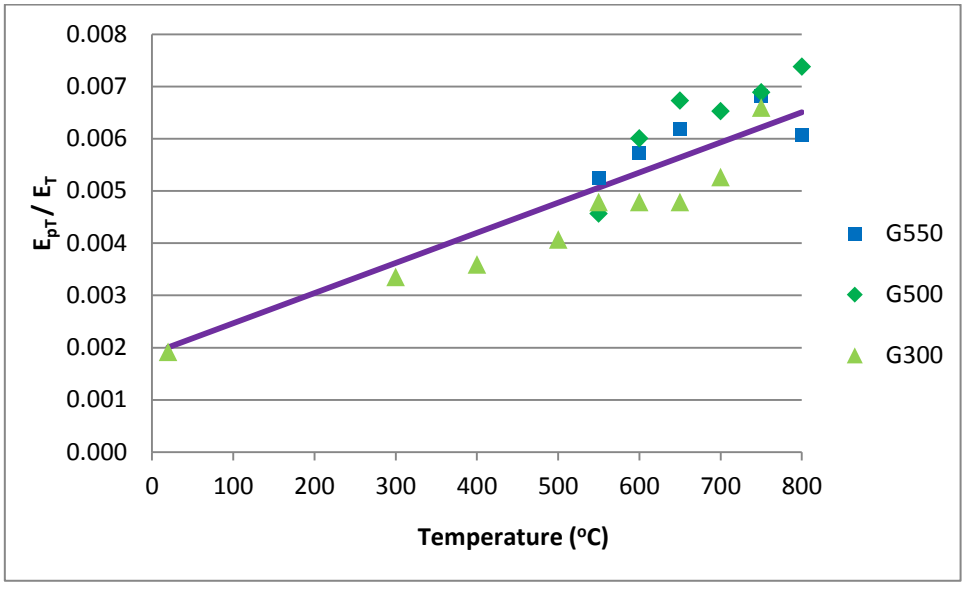

Figure 13: E_{pT}/E_T ratio versus exposed temperature

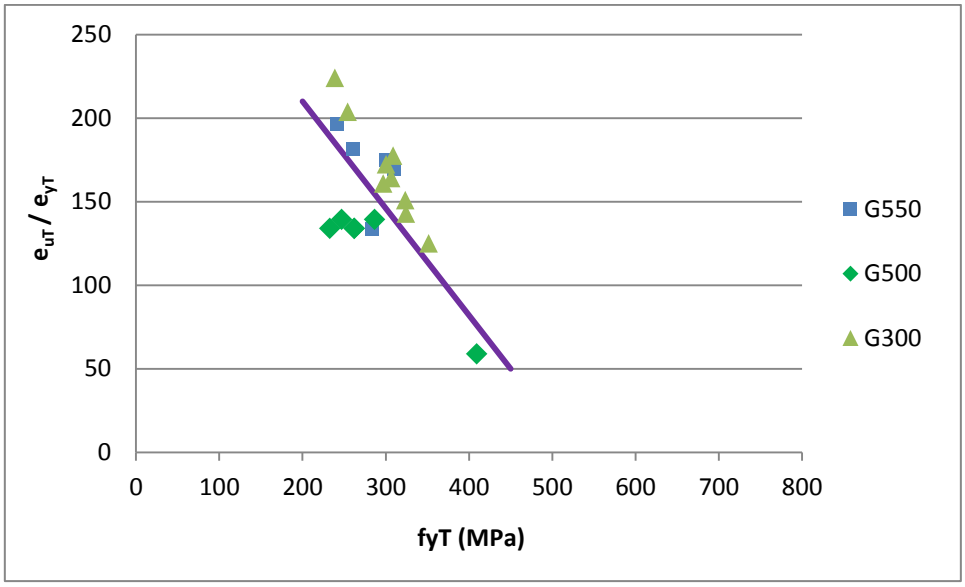

(a) e_{uT}/ e_{yT}

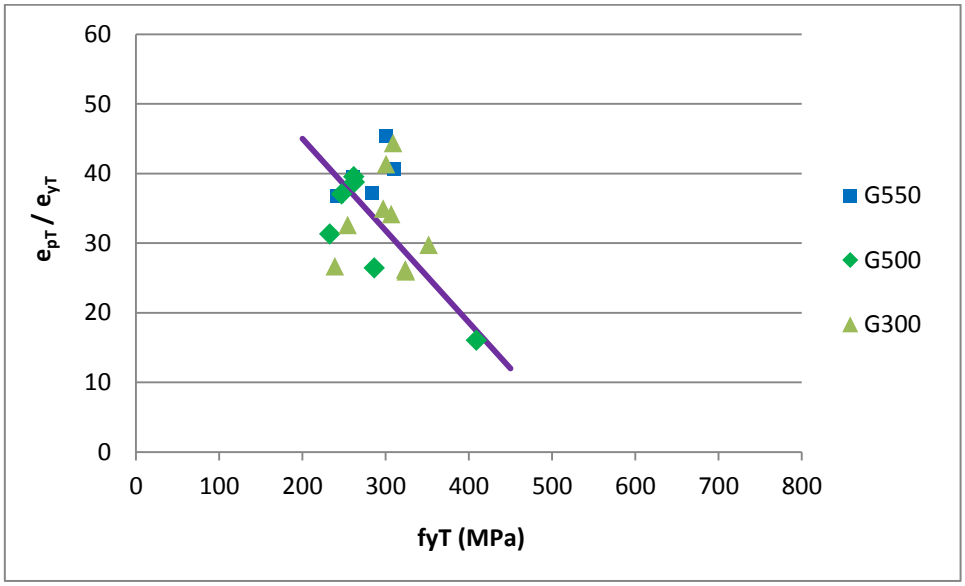

(b) e_{pT}/e_{yT}

Figure 14: e_{uT}/ e_{yT} and e_{pT}/e_{yT} ratios versus yield strength f_{yT}

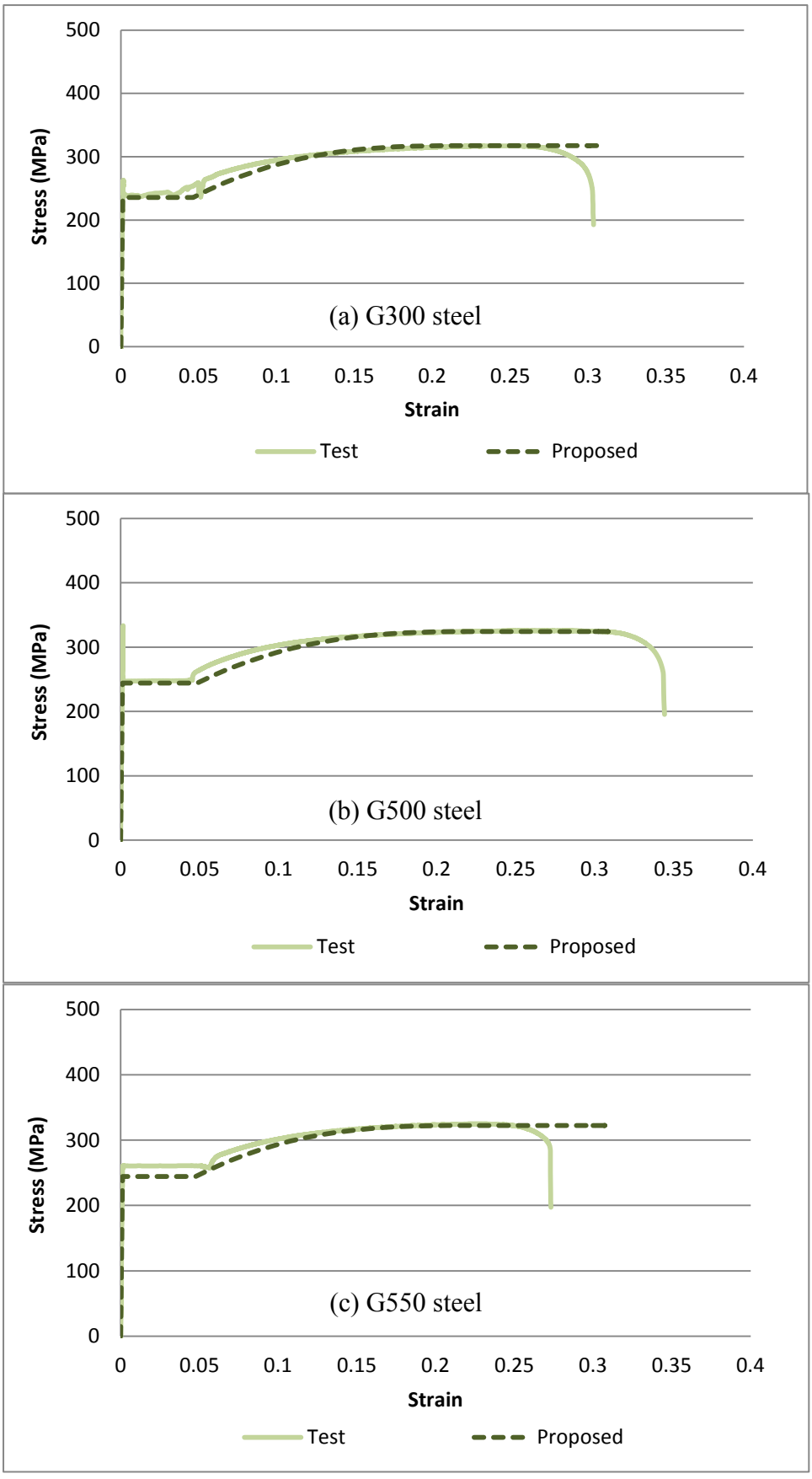

Figure 15: Comparison of stress-strain curves for an exposed temperature of 750 ^{o}C

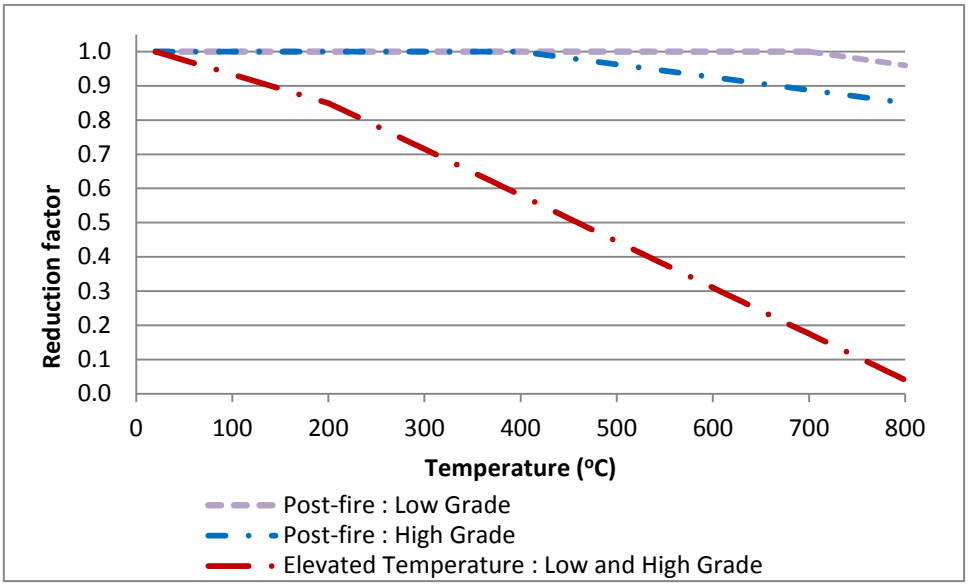

(a) Elastic modulus

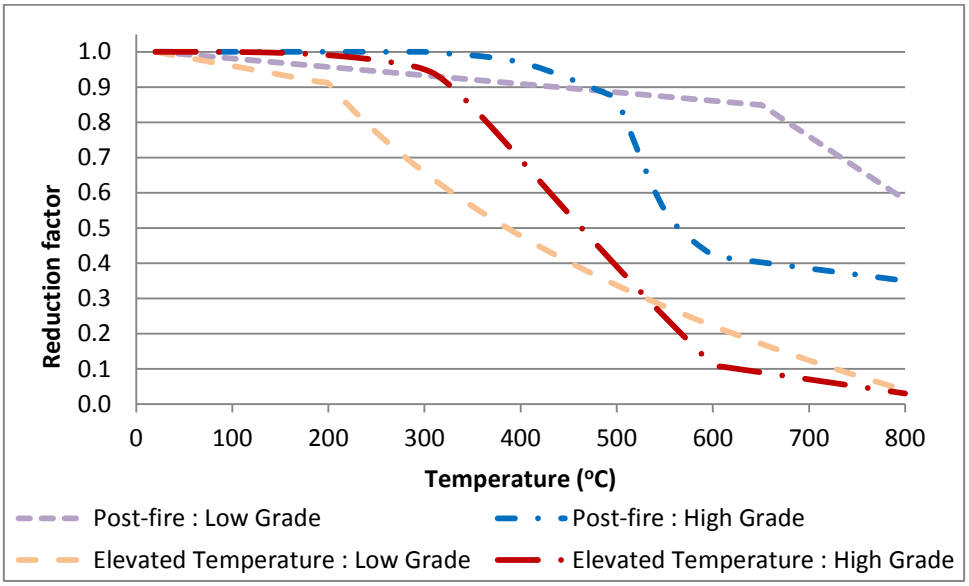

(b) Yield strength

Figure 16: Reduction factors at elevated temperatures and after cooling down

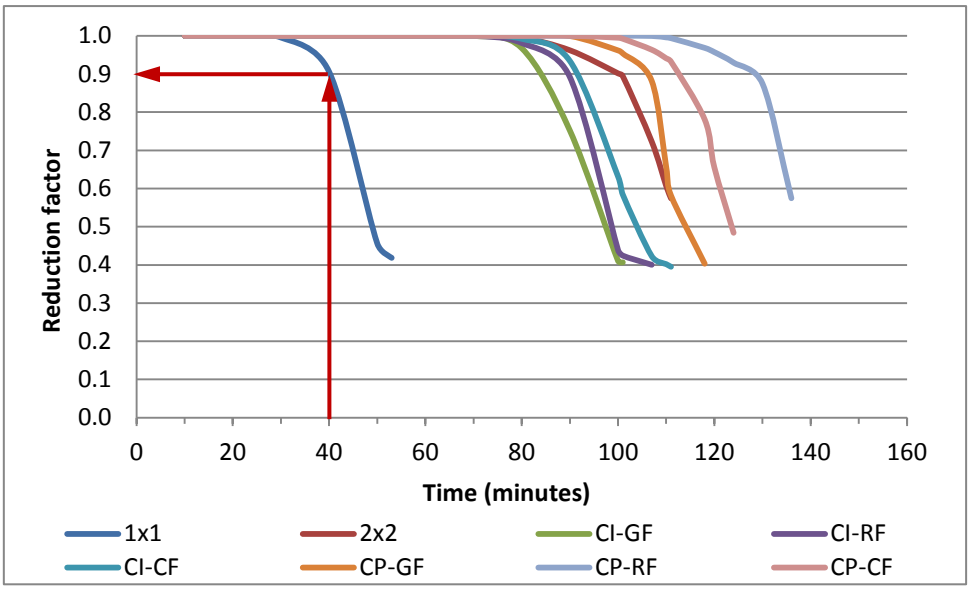

Figure 17: Post-fire yield strength reduction factors for G500-1.15 mm steel studs used in different LSF wall configurations